BIOCHEMICAL AND BIOPHYSICAL RESEARCH COMMUNICATIONS **233,** 238–243 (1997)
ARTICLE NO. RC976438

A Radiobiological Probe for Simultaneous NMR Spectroscopy and ^{192}Ir Gamma Irradiation of *Saccharomyces cerevisiae*

Jennifer E. Magness and Eric W. McFarland[1]
Department of Chemical Engineering, University of California, Santa Barbara, Santa Barbara, California 93106-5080

Received March 7, 1997

A novel nuclear magnetic resonance (NMR) spectroscopy probe was designed and constructed for the study of transient metabolic changes in cellular systems during exposure to ionizing radiation. The probe incorporated a bioreactor, a radiation source, and a radiofrequency detection circuit tunable between 100 and 300 MHz for *in vivo* NMR spectroscopy of ^{23}Na, ^{13}C, and ^{31}P at 11.7 Tesla. The bioreactor system allowed perfusion, oxygenation, and temperature control of cultured cells during irradiation and while performing simultaneous spectroscopic experiments. The concentric design of the bioreactor allowed for the insertion of a ^{192}Ir gamma ray source (E_γ = 370 keV) to allow irradiation of the bioreactor system during the acquisition of NMR spectra. Initial results of ^{31}P spectra obtained during simultaneous gamma irradiation of *Saccharomyces cerevisiae* at approximately 8 Gy/hr show rapid decreases in adenosine triphosphate (ATP) and polyphosphate at the onset of irradiation followed by a slow recovery of polyphosphate. © 1997 Academic Press

Magnetic resonance has become an established and routinely utilized method for study of *in vivo* metabolism (1). Extensive studies of yeast using both ^{13}C and ^{31}P NMR have been published together with techniques to allow continuous perfusion of the cells with nutrients and oxygen during the NMR acquisition (2,3). These methods have allowed the glycolytic rates of cells utilizing several energy sources to be studied and the relative concentrations of adenosine triphosphate (ATP), adenosine diphosphate (ADP), and inorganic phosphate (P_i) to be monitored (4). Furthermore, ^{31}P NMR spectroscopy is a convenient method for determining the intracellular and extracellular pH using the chemical shift of the inorganic phosphate resonance (5,6). To date, magnetic resonance studies in radiation biology have been limited to post-irradiation metabolic evaluations.

Understanding the direct and indirect effects of ionizing radiation on cellular metabolism remains a major challenge in radiobiology. To date, metabolic changes due to ionizing radiation have been measured "immediately after" irradiation because no method has existed to monitor metabolites, *in vivo*, during the actual irradiation. Post-irradiation metabolite content has been widely studied by NMR and other methods (7-9). Holahan *et al.* showed that recovery rate depended on liquid holding media and original dose received by the cells (9). In the same study, it was also observed that polyphosphates were hydrolyzed as a source of phosphates for repair of radiation damage. These studies were performed up to 48 hours after the irradiation with high doses. In studies on mouse leukemia cells, the relationship between the ATP-β peak before and after irradiation was correlated with the dose deposited in the cell culture (10). This effect is thought to be due to cell death and the removal of ATP from the total ATP pool. In all previous studies, only cumulative changes or late effects in cells due to radiation damage have been characterized. The goal of our work was to develop an experimental method that couples the non-invasive power of NMR spectroscopy with simultaneous cellular irradiation to investigate acute, transient changes in cellular metabolism. We developed our probe system to provide a means of performing simultaneous irradiation and metabolic monitoring by NMR spectroscopy.

Saccharomyces cerevisiae have long been the subject of radiobiological studies and an extensive literature has been established. The LD_{50} for anoxic and oxygenated cells are 750 and 250 Gy, respectively (11). Studies have been done on the effect of heavy ions on yeast colony-forming ability post-irradiation (12), on double strand breaks in radiosensitive yeast strains (13), and on the radical formation (14). Characterization of changes in yeast membrane structure and function from ionizing radiation has also been reported (15,16).

[1] Corresponding author. Fax: (805) 893-4731. E-mail: mcfar@engineering.ucsb.edu.

0006-291X/97 $25.00

As in mammalian cells, the bioenergetics of yeast depend upon the high-energy phosphate pathways involving the NMR visible ATP, ADP, and P_i in glycolysis and oxidative metabolism. In addition, both long and short chain polyphosphates are important as both a reservoir for phosphate bond energy (analogous to creatine phosphate in mammalian cells) and as a direct energy source. Two systems for the synthesis of short to medium chain polyphosphates have been elucidated. The first involves phosphate transfer by polyphosphate phosphotransferase from ATP and the second uses diphosphoglycerate as the source of phosphate. The second reaction is important as an alternative storage for high energy phosphate bonds during glycolysis. It has been proposed that the long chain polyphosphates located in proximity to the cell wall are created during the synthesis of cell wall mannoproteins (17). It has also been proposed that these long chain polyphosphates are integral to a transport-associated phosphorylation of glucose (18).

Repair mechanisms for radiation damage are energy consuming. In yeast ATP, polyphosphates and the high energy phosphate pathways are known to be involved in providing energy for repair (9). These pathways can be specifically monitored using ^{31}P NMR spectroscopy. One question we asked was what specific changes occur in phosphate metabolite concentration immediately after commencing irradiation. We hypothesized that a change in ATP would occur as repair mechanisms were followed by a decrease in polyphosphates corresponding to a restoration of steady state ATP levels. These changes would be analogous to the changes in ATP and creatine phosphate during transient stimulation of muscle (19,20).

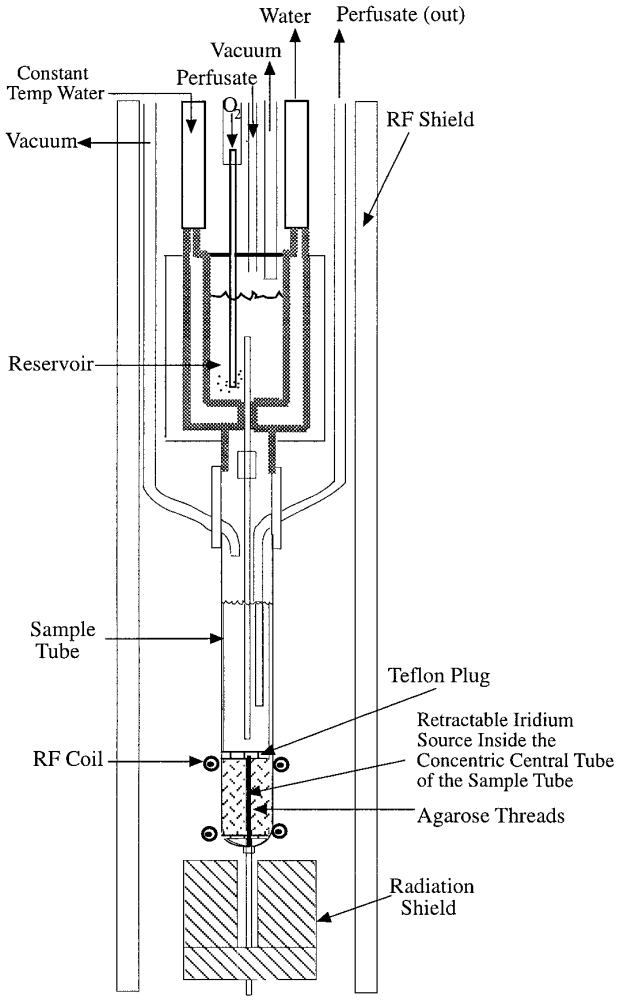

FIG. 1. Probe system schematic. Fresh cell perfusate enters the probe reservoir from an external supply and is oxgenated. The reservoir is surrounded by a temperature controlled brass water jacket and feeds the bioreactor below through a central tube. The bioreactor liquid level is maintained by the outflow pumping speed. Both the reservoir and bioreactor have overfill levels protected by tubes connected to vacuum suction. The cells are contained in the lower quarter of the bioreactor tube by permeable plugs. For irradiation, the ^{192}Ir source is raised from the shielded compartment below the probe up into the concentric central cavity of the bioreactor tube.

MATERIALS AND METHODS

Probe design. A prototype NMR probe system was designed and built for simultaneous irradiation and metabolic spectroscopy. The probe system consisted of three subsystems: 1) a radio frequency coil and resonant circuitry for NMR signal detection, 2) a concentric glass bioreactor and cell perfusion assembly, and 3) a moveable ^{192}Ir source and shielding. Figure 1 shows schematically the three subsystems.

The r.f. detection system included an LC resonant circuit (tuned to 202 MHz for ^{31}P with a saddle coil constructed of copper foil around a 25 mm o.d. glass tube. The saddle coil was 4.15 cm in length with inductance 0.36 μH constructed for optimal field homogeneity and geometrical constraints. The quality factor of the empty coil was 202 while the quality factor of the coil loaded with 32 mM phosphoric acid was 135. The sensitivity of the probe was tested by measuring the signal-to-noise ratio (SNR) of the Fourier transform of a single free induction decay (FID) from various concentrations of phosphoric acid following a single 90 degree pulse. The SNR of the Fourier transformed FID from a single pulse varied linearly with phosphate concentration with a slope of approximately 85 M^{-1}.

The bioreactor subsystem was designed to allow perfusion and temperature control of the cells during irradiation and spectroscopy. The cells supported within agarose threads were contained in a 20 mm o.d. quartz tube with a concentric 5.0 mm central tube which allowed insertion of the gamma source from below. The cell/agarose matrix was perfused with the same phosphate buffer described above with the addition of 50 mM glucose. The sample tube containing the gel threads was suspended from a glass reservoir of phosphate buffer which was itself suspended in a plastic cylindrical support structure inside the bore of the magnet.

The reservoir temperature was controlled by a brass water jacket through which temperature-regulated water was pumped, maintaining a temperature of 30°C. The small reservoir in the magnet was fed by a larger reservoir outside the magnet, using a peristaltic pump (Biochem Technology). The total volume of buffer in the perfusion system was approximately 1 L. The flow rate of perfusate was 200 mL/hr. Oxygen was bubbled through the buffer in the magnet reservoir. The buffer was gravity fed from the magnet reservoir to a level just above the cell culture and was removed from the NMR tube by an outlet tube connected to another peristaltic pump. The outlet tube was 5 cm above the agarose threads, and a Teflon plug with small holes above the threads prevented the cell matrix from

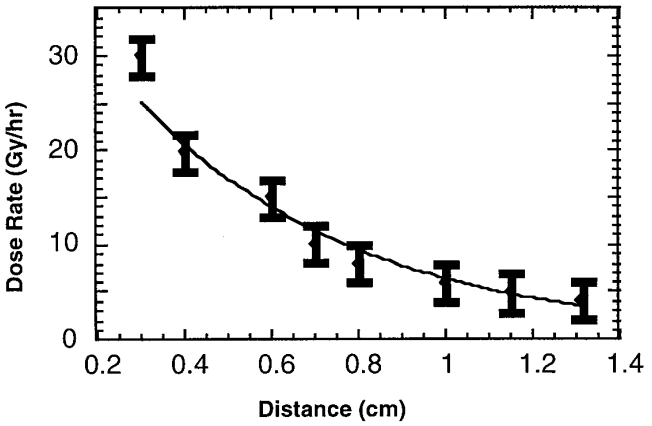

FIG. 2. Measured dose rate at several radial distances from a single cylindrical ^{192}Ir seed (activity ~11 mCi).

being removed from the NMR tube. Both the NMR tube and the magnet reservoir were prevented from overflowing by attaching a vacuum safety system to both.

The radiation source was ^{192}Ir in the form of platinum-coated pellets, "seeds," which were encased in a thin wall aluminum tube to create a 1.5 mm diameter line source in the center of the 20 mm NMR sample tube, Figure 1. A copper shielded source isolation chamber was located below the sample tube. Copper was chosen because of its minimal magnetic susceptibility and high atomic number. The radiation source was enclosed in the shielded isolation chamber while control (no irradiation) spectra were obtained, then inserted into the central concentric tube during cell system irradiation. Copper rotating doors sealed the top of the source isolation chamber. The doors could be opened and the source moved into the sample area without removing the probe from the magnet. The decay of ^{192}Ir generates several different energy gamma-ray photons with an average energy of 370 keV. The half-life is 74.2 days with an average of 2.2 gammas emitted per decay. The activity required to produce 5 Gy/hr at 10 cm was calculated to be approximately 185 mCi after accounting for the characteristics of the line source and the decay constant of ^{192}Ir over the course of the experiments. The measured dose rate for a single ^{192}Ir seed at several distances is shown in Figure 2. Using this data, the volume-averaged dose rate was calculated for all 11 seeds to be approximately 8.0 Gy/hr. The actual dose deposited in the cells was recalculated for each experiment from the known half-life.

Cells. Wild-type *Saccharomyces cerevisiae* (strain AC502) were acquired on agarose plates from the Department of Biological Sciences, University of California at Santa Barbara. The method of cell preparation was similar to that described by Brindle and Krikler (3). Cells were grown aerobically in a medium consisting of 5 g yeast extract, 10 g peptone, 25 mg uracil, 25 mg adenine, 10 g dextrose, and 500 mL deionized water. The cells were incubated in a gyratory shaker at 90-110 rpm for 15 to 20 hours at a constant temperature of 30°C and harvested in mid-log phase.

Cell density was determined using a spectrophotometer, with the optical density measured and calibrated to the actual density of cells in the broth. Before cell collection, the cells were cooled to approximately 4°C in an ice bath. The cells were harvested by low-speed centrifugation at 5000 rpm for 10 minutes at 4°C, then washed once in 500 mL of an ice-cold phosphate buffer. This buffer contained 116 mg KH_2PO_4, 26 mg K_2HPO_4, 120 mg $MgSO_4$, 50 mg NaCl, 4.88 g MES (2-[N-Morpholino] ethanesulfonic acid: Sigma), and 500 mL water with the pH adjusted to 6.0 using 1 M NaOH. After being washed, the cells were centrifuged again at the same speed, duration, and temperature, and the pellet was brought up to room temperature. Cell suspension was then mixed with 10 mL of 1.8% low gelling temperature agarose, which had been dissolved in the phosphate buffer and brought to room temperature.

The cell/agarose mixture was extruded with a 22 gauge syringe through approximately 0.75 m of Tygon tubing (800 μm inner diameter), which was cooled in an ice/water bath. The extruded gel threads were collected in the 20 mm quartz bioreactor tube containing 15 mL ice-cold buffer. The total sample volume was 14 mL with a cell density of approximately 10^8 cells/mL.

The first set of experiments were performed without perfusion, with the aerator inserted directly into the NMR sample tube. Antifoam A (Sigma) was added to the suspension medium in these experiments to prevent the formation of large bubbles in the NMR tube. Twenty percent (20%) glucose solution (2 mL) was added to the cell sample directly prior to NMR observation. The non-perfused experiments were repeated three times. The second set of six experiments was performed with a perfusion system to renew the phosphate buffer and provide a glucose source.

Magnetic resonance. NMR experiments were performed using a Chemagnetics 500 MHz spectrometer interfaced to a 11.7 Tesla Magnex wide-bore (89 mm diameter) superconducting magnet. ^{31}P spectra were obtained from the Fourier transform of the free induction decay acquired following a single r.f. excitation. Phase cycling and signal averaging were utilized. Five hundred twelve (512) acquisitions were averaged for the non-perfused experiments and 256 acquisitions averaged for the perfused experiments. A repetition time of 1 second and a pulse angle of 71 degrees were used for optimal SNR. Methylene diphosphonic acid (MDP) of 0.1 M concentration was placed in a capillary tube within the NMR sample tube and used as the reference standard. Shimming was performed on 1.6 M phosphoric acid with the radiation source both raised and lowered. The presence of the source in the sample coil introduced approximately 5 Hz of line broadening that could not be shimmed out; the pulse width did not change. The data was analyzed using commercial software. Peak heights were extracted from the spectra and plotted versus time. Peaks were identified by comparison to previous studies (3,21). At one-second repetition times and 71 degrees flip angles, partial saturation of several species was expected. Since relative metabolite changes were of interest (not absolute), no corrections were applied to the results.

RESULTS AND DISCUSSION

In Figures 3(A) and 3(B), spectra of control and irradiated cell preparations are shown, respectively, in the absence of perfusion. The marked ^{31}P resonances are the methylene diphosphonate indicator, MDP (1), sugar phosphates (2), inorganic phosphate (intra- and extracellular) (3), ATP-γ (4), ATP-α (5), ATP-β (6), and long chain polyphosphates (7). The ATP ^{31}P resonances 4, 5, and 6 are readily identified. The ^{31}P resonances of ADP and AMP overlap with ATP at 4 and 5, and 5, respectively. Only the ATP-β peak uniquely monitors ATP. In the control preparations, Figure 3(A), high energy phosphates were still observable after 300 minutes. All three ATP phosphate peaks were still measurable in the control cells indicating that both ATP and ADP were available in the cells. Polyphosphate was also visible in the control cells after 300 minutes, peak 7. In the irradiated cells, Figure 3(B), the resonances corresponding to the presence of ADP and ATP (peaks 4 and 6) were significantly reduced after 300 minutes. In particular, the unique ATP-β peak is not measur-

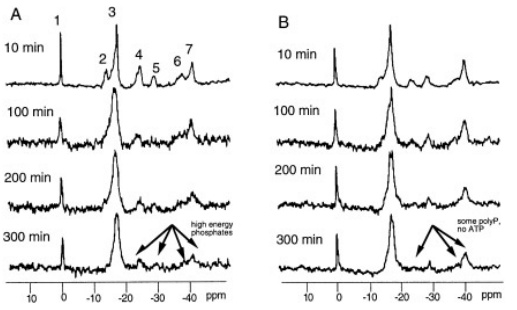

FIG. 3. Spectra of non-perfused cells (A) without irradiation and (B) during irradiation. The peaks are as follows: (1) methylene diphosphonate (MDP) - reference standard, (2) sugar phosphates, (3) inorganic phosphate (internal and external), (4) ATP-γ and ADP-β, (5) ATP-α and ADP-α, (6) ATP-β and short chain polyphosphates, and (7) long chain polyphosphates. In (A), after 300 minutes, it appears that high energy phosphates such as ATP and ADP remain. However, in (B) the peaks corresponding to the second and third phosphates of ATP are almost unobservable. The average dose rate for the irradiated cells was 8.64 Gy/hr.

able. Peak 5, possibly corresponding to AMP, was present as well as polyphosphate (peak 7). The ratios of ATP-β and polyphosphate were followed; and although they appeared qualitatively different, no statistically significant difference was found for at least 2.5 hours.

In the second group of experiments, cells were maintained at approximately steady state metabolic conditions with the nutrient perfusion system. Figure 4 shows spectra from control and irradiated cell samples at different times during the experiment. In Figure 4(A), the metabolites in the control cells are shown to be stable for the duration of the experiment. Figure 4(B) shows typical spectra from irradiated cells. Repeat spectra over one hour prior to irradiation show the cells to be stable and similar to controls. Within minutes after beginning irradiation, decreases in the ATP-β and polyphosphate occurred.

Figure 5 shows the time course of ATP-β for the control and irradiated samples. In control samples, all of the high energy phosphates varied no more than 15%

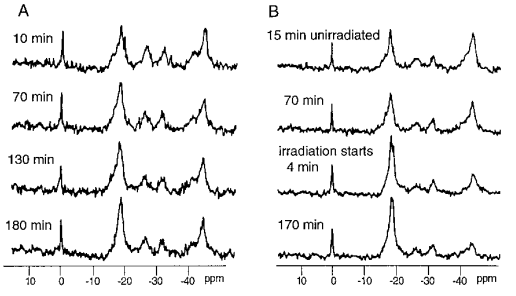

FIG. 4. Spectra of perfused cells during irradiation. In (A), the unirradiated cells maintain relatively constant amounts of the high energy phosphates ATP and polyphosphate. In (B), once irradiation has begun, the peak heights of ATP-β and polyphosphate decrease by an average of approximately 30%.

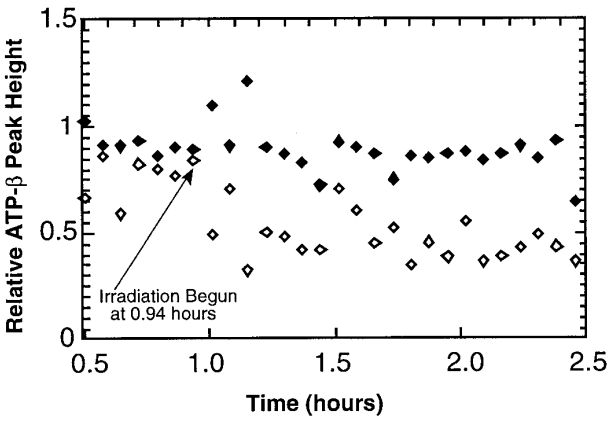

FIG. 5. Changes in ATP-β in perfused cells. The ATP-β peak heights for irradiated (◇) and control (◆) cell samples are plotted versus time relative to the initial peak height from a single experiment. The irradiation was started approximately 1 hour after NMR observation began. Once the irradiation began, the ATP-β peak decreased and remained at a lower value for the remainder of the experiment. The average dose rate for the irradiated cells was 7.94 Gy/hr. Each data point has an error in peak height determination of approximately ±15% based on the signal-to-noise ratio.

over the course of an experiment. In the irradiated samples, immediately after the onset of irradiation the ATP-β, peak decreased by an average of 28%. This decrease was observed for the duration of the experiment. In Figure 6, the changes in the polyphosphate peak height are shown. At the onset of irradiation, the polyphosphate peak dropped to 32.8% of its original value. With continued irradiation, this resonance returned slowly to approximately 64.2% of its initial value.

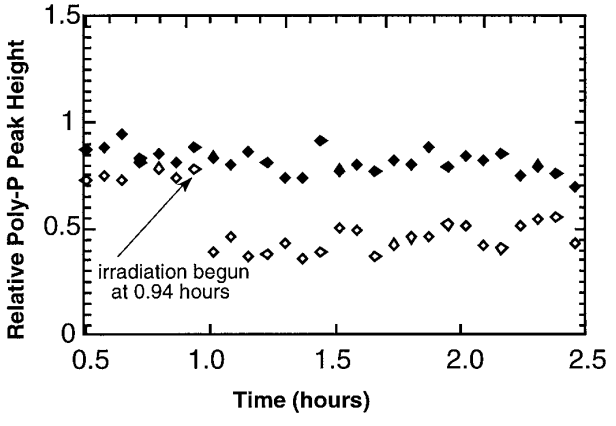

FIG. 6. Changes in polyphosphate in perfused cells. The polyphosphate peak heights for irradiated (◇) and control (◆) cell samples are plotted versus time relative to the initial peak height from a single experiment. The irradiation was begun approximately 1 hour after NMR observation began. A large decrease in polyphosphate occurred within the first few minutes of irradiation. The average dose rate for the irradiated cells was 7.94 Gy/hr. Each data point has an error in peak height determination of approximately ±15% based on the signal-to-noise ratio.

In the experiments without bioreactor perfusion our hypothesis was that the irradiated cells would exhaust high energy phosphates, ATP and polyphosphate, more rapidly than the control samples as they increased their metabolic needs for the repair of radiation induced damage (9). This hypothesis was qualitatively supported by our results; however, further work would be required to reach statistical significance. Similarly, in all irradiated cell samples, ATP (as monitored by the ATP-β resonance) was exhausted more rapidly than the controls although again not enough to achieve statistical significance. One problem encountered in the experiments performed without perfusion was that carbon dioxide from the respiring cells formed bubbles in the cell matrix which introduced susceptibility gradients (at the air-liquid interface) and reduced the SNR due to resonance broadening. In the subsequent experiments where perfusion is implemented, this problem is negligible as perfusion clears the excess carbon dioxide.

The effects of ionizing radiation on cells maintained in a stable nutritional state were best examined in the perfused cell systems. The high energy phosphate peak heights in the stable control samples never deviated from the average more than 15%; therefore, in irradiated samples it was assumed that changes in peak height greater than 15% were due to radiation effects. Decreases in polyphosphate and ATP were observed immediately after irradiation began. The polyphosphate and ATP-β peaks decreased an average of 32.8% and 28.0%, respectively, within the first 4 minutes of irradiation. The average dose at 4 minutes was only 0.6 Gy, well below the dose required to cause observable cell death or critical DNA double strand breakage (7). Therefore, the high energy phosphate compounds may have been utilized to repair acute sublethal radiation damage such as injury to the cell and nuclear membranes caused by free radical ions. The utilization of polyphosphate as well as ATP indicates that the ATP pool alone was inadequate to meet the transient metabolic challenge initiated with irradiation and that reserve energy stores as well as immediate energy sources were required.

There were no immediate noticeable changes in peaks 4 and 5 after the onset of irradiation which is consistent with a concurrent increase in ADP with reduction in ATP and the overlap of ATP-α and -γ with ADP. Only a change in the total nucleotide di- and triphosphate pool can be expected to cause a change in these peak heights. Our results indicate that with irradiation this pool does not change. We did notice over the seven hours a gradual reduction in total nucleotide phosphate and gradual increase in inorganic phosphate (data not shown).

After the initial decrease in polyphosphate, in most experiments the concentration began to increase slowly. The recovery on average was to 64.2% of the original polyphosphate value, up 23.2% from the initial decrease due to radiation. The polyphosphate peak did not return to the original value in any of the data sets. We speculated that either the experiment did not last long enough for full recovery or, more likely, that by the time the cells had been irradiated for 7 hours, the maximum dose received by the cells nearest to the source was above the threshold for observable cell death. One explanation for the slow increase in polyphosphate is an increase in cellular metabolic rate which appeared almost linear with dose in several experiments. This increase in metabolic rate must be significant because the energy of hydrolyzation for the polyphosphate phosphoanhydride bond is equal to that of ATP. Alternatively, the energy requirements for polyphosphate production might be decreasing in time.

In contrast to the recovery of the polyphosphate peak, the ATP-β peak remained decreased for the remainder of the experiment in all cases. This peak is normally low (less than 1 mM concentration) in healthy anaerobic cells, but since oxygen and glucose were not limited in these experiments it is assumed that respiration was taking place in the cells — even after irradiation was begun. An alternative explanation for the reduction in ATP-β peak is that ATP is being utilized to repair radiation damage at the same rate it is being synthesized. Thus, at any given time there would be a decreased total ATP pool and constant nucleotide phosphate.

These preliminary results showing evidence of a rapid increase in cellular metabolic rate immediately after the onset of irradiation came as quite a surprise. At the dose rates utilized, the number of ions produced in the cells during the irradiation based upon the number of primary ionizations per cell is approximately 2.8×10^3 ions/cell/hr. Thus, at 4 minutes into the irradiation, each cell would have been exposed to almost 200 reactive ion species, any of which could lead to sublethal damage and activation of repair mechanisms. Could this number be high enough to trigger a metabolic response? If all the primary ions are summed over an hour, the yield is only 9×10^{-9} M. The only known metabolic trigger that appears to be as sensitive is that of pH. If the secondary ions produced from the radical species are considered, the concentration of ions over one hour would increase; however, the actual number would depend highly upon the availability of scavengers.

Extension of our preliminary studies will include investigations on radiation sensitive (rad 52) mutant yeast strains (LD_{50} in O_2 is 25 Gy and in N_2 75 Gy). We expect larger and longer shifts in phosphate metabolites in these isolates because of their lack of immediate repair mechanisms. In addition, more complete media (including a nitrogen source) will be utilized to eliminate metabolic stress effects. Although significant cell death is not expected even in the regions of highest dose, cell counts pre- and post-irradiation and perfu-

sion will be performed to insure against significant population shifts.

In summary, we have described a novel radiobiology probe for NMR spectroscopy and have shown that the combination of NMR spectroscopy and simultaneous cellular irradiation may be a valuable technique for the study of radiation effects on cellular metabolism. Our initial results with this device support a rapid increase in the cellular metabolic rate and requisite decrease in high energy phosphate metabolites following the onset of cellular irradiation. Though not yet statistically significant, the findings are evidence for a sensitive metabolic trigger induced by low dose ionizing radiation and demonstrate the potential usefulness of this system.

ACKNOWLEDGMENTS

This research was supported by the Cottage Hospital Research Fund and NSF Grant DIR91-96193. The authors thank A. E. Profio, D. Parker, and J. Casto for many helpful discussions and for their assistance in the selection and handling of the source, D. Parker for dose rate distribution calculations, K. Middleton and the workers in Professor J. Carbon's Lab for help with the cell samples, M. A. Jimenez for assistance with the perfusion system, and T. Hedger and others from Alpha-Omega Services, Inc. (Bellflower, CA) for assistance in assembling the radiation source. We are grateful to Pat White for her help in the preparation of the manuscript.

REFERENCES

1. Shulman, R. G., *et al.* (1979) *Science* **205,** 160–166.
2. Jacobson, L., and Cohen, J. S. (1981) *Bioscience Reports* **1,** 141–150.
3. Brindle, K. M., and Krikler, S. (1985) *Biochim. Biophys. Acta* **847,** 285–292.
4. Brindle, K. M. (1988) *Biochem.* **27,** 6187–6196.
5. Moon, R. B., and Richards, J. H. (1973) *J. Biol. Chem.* **248,** 7276–7278.
6. Barton, J. K., *et al.* (1980) *Proc. Natl. Acad. Sci. USA* **77**(5), 2470–2473.
7. Frankenberg-Schwager, M., *et al.* (1980) *Rad. Research* **82,** 498–510.
8. Fingerhut, R., *et al.* (1980) *Radiat. Environ.* **18,** 19–26.
9. Holahan, P., *et al.* (1988) *Int. J. Radiat. Biol.* **54**(4), 545–562.
10. Ulmer, W. (1990) *Radiobiol. Radiother.* **31,** 313–323.
11. Boreham, D. R., and Mitchel, R. E. J. (1991) *Rad. Research* **128,** 19–28.
12. Schoepfer, F., *et al.* (1982) *Rad. Research* **92,** 30–46.
13. Ho, K. (1975) *Mut. Research* **30,** 327–334.
14. Teebor, G. W., *et al.* (1988) *Int. J. Radiat. Biol.* **54**(2), 131–150.
15. Khare, S., *et al.* (1982) *Int. J. Radiat. Biol.* **42**(4), 369–383.
16. Leyko, W., and Bartosz, G. (1986) *Int. J. Radiat. Biol.* **49**(5), 743–770.
17. Kulaev, I. S., *et al.* (1987) *in* Phosphate Metabolism and Cellular Regulation in Microorganisms (A. Torriani-Gorini *et al.,* Eds.), pp. 233–238, Am. Soc. Microbiol., Washington, DC.
18. Van Steveninck, J., *et al.* (1987) *in* Phosphate Metabolism and Cellular Regulation in Microorganisms (A. Torriani-Gorini *et al.,* Eds.), pp. 239–244, Am. Soc. Microbiol., Washington, DC.
19. Meyer, R. A., Brown, T. R., and Kushmerick, M. J. (1985) *Am. J. Physiol.* **248** (Cell Physiol. 17): C279–287.
20. McFarland, E. W., Kushmerick, M. J., and Moerland, T. S. (1994) *Biophys. Journal* **67,** 1912–1924.
21. Den Hollander, J. A., *et al.* (1981) *Biochem.* **20,** 5871–5880.